Microfluidic Porous Silicon Aptasensor Array for Multiplex Detection of Sepsis Biomarkers Using Reflectometric Interference Fourier Transform Spectroscopy (RIFTS)

Sh. Mohammadi[1], F. Rahimi[1*], A.H. Rezayan[1], A. Abouei Mehrizi[2] and M. Sedighi[3,4]

[1] Department of Nanobiotechnology and Biomimetics, School of Life Science Engineering, College of Interdisciplinary Science and Technology, University of Tehran, Tehran, Iran.
[2] Department of medical technology and tissue engineering, School of Life Science Engineering, College of Interdisciplinary Science and Technology, University of Tehran, Tehran, Iran.
[3] Cellular and Molecular Research Center, Birjand University of Medical Sciences, Birjand, Iran
[4] Department of Nanomedicine, Faculty of Medicine, Birjand University of Medical Sciences, Birjand, Iran

ABSTRACT

Multiplexing in point-of-care biosensors has revolutionized diagnostics across various fields, including medicine, environmental monitoring, and the food safety, by enabling rapid and simultaneous analysis of multiple analytes. In clinical settings, this technology is particularly crucial for multifactorial, multistage, and potentially fatal conditions like sepsis, a major cause of mortality in intensive care units. Consequently, the development of rapid, accurate, and multiplexed detection methods for sepsis-related biomarkers is crucial for timely diagnosis and informed treatment decisions. Herein, we present a novel label-free aptasensor platform based on porous silicon employs Reflective Interferometric Fourier Transform Spectroscopy (RIFTS), utilizing a 3-channel microfluidic system to multiplex detection of three sepsis biomarkers: C-reactive protein (CRP), tumor necrosis factor-alpha (TNF-α), and interleukin-6 (IL-6). The selectivity of the developed sensing platform was cross-validated versus commonly known interfering non-target proteins without compromising its performance values and in the clinical range of severe sepsis. This innovative approach offers potential for rapid, sensitive, and specific multiplex detection of biomarkers potentially improving patient outcomes through comprehensive and more accurate diagnosis.

Keywords: Multiplex- Microfluidic- RIFTS- Silicon- Aptasensor- Biomarker- Reflectometric.

1. *INTRODUCTION*

Biosensor technology has emerged as a promising solution to address the limitations of conventional assays, offering a range of advantages that make it particularly well-suited for advanced diagnostic applications. These benefits include enhanced sensitivity and selectivity, the capability for continuous measurement, rapid response and analysis times, robust performance, potential for miniaturization towards lab-on-chip technologies, and high reproducibility. This approach not only enhances patient care by ensuring more effective treatments with fewer side effects but also makes advanced diagnostics accessible in resource-limited settings[۱].

Multiplex detection in point-of-care (POC) biosensors has emerged as a transformative approach in diagnostics, offering rapid, cost-effective, and simultaneous analysis of multiple biomarkers. Beyond healthcare, multiplex POC biosensors are finding applications in environmental monitoring, where they can simultaneously detect multiple pollutants or pathogens in water and soil samples[۲, ۳]. In the food industry, these sensors offer rapid on-site detection of contaminants, allergens, and adulterants, enhancing food safety measures throughout the supply chain. Multiplex POC biosensors enable comprehensive disease profiling, early diagnosis, and personalized treatment strategies by detecting multiple analytes in a single test[۴, ۵].

These devices have shown particular promise in diagnosing and managing complex, multifactorial, and multistage diseases such as sepsis, a life-threatening condition caused by a dysregulated host response to infection, remains a global health challenge. While no single ideal biomarker exists for sepsis, a panel approach has emerged as the preferred diagnostic method, particularly for point-of-care (POC) testing[۷, ۶]. Among the most extensively studied potential biomarkers are tumor necrosis factor-alpha (TNF-α) and interleukin-6 (IL-6), pro-inflammatory cytokines that play crucial roles in initiating SIRS, as well as C-reactive protein (CRP), an acute phase reactant synthesized in the liver in response to IL-6 stimulation.

In the early stages of sepsis, these biomarkers begin to rise, reflecting the body's inflammatory response to infection. CRP levels typically increase to 50–200 µg/mL, TNF-α to 20–100 pg/mL, and IL-6 to 100–1,000 pg/mL. Each of these biomarkers plays a unique role in the sepsis cascade. CRP, an acute-phase reactant produced by the liver, serves as a non-specific marker of inflammation, with levels increasing within 6–12 hours and peaking at 48 hours. TNF-α, a pro-inflammatory cytokine, initiates the inflammatory cascade and acts as an early marker of sepsis, with high levels correlating with disease severity. IL-6, another pro-inflammatory cytokine, amplifies the immune response and rises rapidly within hours of infection, serving as a sensitive marker for early sepsis detection[۷, ۶]. The combined elevation of these biomarkers, especially when accompanied by clinical signs such as fever, tachycardia, and hypotension, strongly supports the diagnosis of sepsis. Moreover, extremely elevated levels of TNF-α and IL-6 are strong predictors of poor outcomes, including multi-organ failure and increased mortality. This multi-marker approach holds promise for improving sepsis outcomes across a wide range of clinical scenarios, from early detection to monitoring treatment efficacy[8].

Among the various biosensor configurations, Fabry-Pérot interferometers fabricated from porous nanomaterials such as silicon, have garnered significant attention in the development of effective optical biosensing platforms. The appeal of these structures lies in their inherent tunable characteristics, which confer several advantages over competing methods. These include a high surface area-to-volume ratio (500−800 m^2/cm^3) for increased sensitivity, straightforward fabrication processes, and tunable optical and physical properties that enhance overall device performance. The optical properties of porous thin films in these interferometers are typically measured in real-time using techniques such as reflective interferometric Fourier transform spectroscopy (RIFTS)[9, 10]. RIFTS method is extremely sensitive to refractive index variations, allowing for precise detection of analyte binding events or changes in the local environment within the porous structure. Despite the potential of optical detection systems for protein and DNA targets, their performance has been hindered by relatively high detection limits, typically in the micromolar range for direct and label-free approaches. Microfluidic integration with biosensors is revolutionizing lab-on-a-chip platforms[9, 11]. This combination miniaturizes systems, reducing sample volumes and analysis times while enabling high-throughput, portable, and cost-effective detection. Importantly, microfluidics enhances mass transfer to biosensor surfaces, significantly improving sensitivity and mass transfer compared to traditional methods. This advancement is driving the development of more efficient and accessible diagnostic tools for various scientific and medical applications.

Herein, we present a label-free aptasensor platform based on porous silicon, utilizing a 3-channel microfluidic system. The platform employs RIFTS to simultaneously identify CRP, TNF-a and IL-6 biomarkers. As a proof of- concept to demonstrate the biosensing capabilities of the platform, oxidized PSi Fabry-Pérot thin film were laser cut and each piece was assigned to bioconjugation a specific aptamer for each biomarker and placed inside the 3-channel chip. A microcontroller-programmed motorized xyz stage was used to control and precisely move the reading points in/between each channel, allowing real-time monitoring. The aptasensor was then exposed to concentrations of samples containing CRP, TNF-α, and IL-6 biomarkers, both individually and in combination.

2. *MATERIALS AND METHODS*

2.1 Materials.

Si wafers (p^+-type, heavily boron doped, 1-9 mΩ·cm-1 resistivity, <100>-oriented) were purchased from Latech Scientific Supply (Singapore). Aqueous Hydrofluoric acid (HF) (48%) and ethanol absolute were purchased from Merck (Germany). (3-aminopropyl) triethoxysilane (APTES), glutaraldehyde 25% (GA), H_2O_2 (35%, v/v) was purchased from Merck (Germany). Additional buffers were phosphate buffered saline (PBS, 1 mM phosphate buffer, 154 mM NaCl2, pH 7.4) and 4-(2-hydroxyethyl)-1- piperazineethanesulfonic acid) (HEPES), which were prepared according to standard recipes with deionized and filtered prior to use. Polydimethylsiloxane (PDMS) was purchased from Dow Corning Sylgard® 184 Silicon Elastomer kit (USA). The CRP specific DNA aptamer (5′-NH_2-ACACGATGGGGGGGTATGATTTGATGTGGTTGTTGCATGATCGTGG-3′), TNF-α specific DNA aptamer (5′-NH_2-TGGTGGATGGCGCAGTCGGCGACAA-3′) and IL-6 specific DNA aptamer (5′-NH_2-GGTGGCAGGAGGACTATTTATTTGCTTTTCT-3′) was purchased from Pishgam Biotech Company (Tehran, Iran) and purified by the BIO-RP purification method. Proteins biomarkers for biosensing experiments included human CRP, TNF-α and IL-6 were purchased from Sigma-Aldrich (Germany).

2.2 Fabrication of PSi.

The wafer cleaning and parasitic layer elimination process were performed according to the previous protocols [12]. In the fabrication of porous silicon (PSi) Fabry-Pérot thin films, a two-step anodic electrochemical etching process was conducted in two stages by a programmable power supply (Rigol DP821, China) was employed. Initially, a parasitic layer was etched for 30 seconds, followed by the main sensing layer, which was etched for 40 seconds. Both stages were performed at a constant current density of 160 $mA{\cdot}cm^{-2}$ and using a 3:1 (v/v) electrolyte solution of hydrofluoric acid (48% HF) and absolute ethanol. Following each etching step, the samples were rinsed with methanol and subsequently dried under a nitrogen gas. The oxidation process of freshly-etched PSi samples were performed as reported previously [12]. Subsequently, the oxidized PSi samples were rinsed in deionized water, dried using a stream of nitrogen gas and laser-cut into pieces of 0.8 × 8 mm^2.

2.3 PSi Surface Modification.

Surface modification of the Si-OH terminated oxidized PSi surface samples, including linker addition APTES, and GA, was carried out according to the previous procedure [12]. The amine terminated aptamers were conjugated onto the surface of the GA activated PSi film by mediated covalent attachment. Successively, the PSi activated surface were incubated with the aptamer solutions one hour at 37°C, in order to allow the immobilized aptamer to properly fold. To minimize the non-specific adsorption, bovine serum albumin (BSA) solution (1 mg/ml) was introduced for 30 min. The resulting aptasensors were washed with PBS buffer (pH = 7.4) and dried under a nitrogen stream.

2.4 Fabrication of Microfluidic Devices.

The described microfluidic chip represents a sophisticated biosensing platform, integrating advanced design, simulation, and fabrication techniques. Designed using SolidWorks 2022 and simulated with COMSOL 6.2, the chip features a single inlet that evenly distributes flow into three parallel channels, each with a dedicated aptasensor chamber. The device is constructed from two precisely micromilled Poly(methyl methacrylate) (PMMA) layers, with the bottom layer housing microchannels and aptasensor chambers and the top layer, which houses the inlet and outlets. The sealing method, combined with the PDMS layer, addresses common challenges in microfluidic device assembly, such as achieving uniform sealing pressure, preventing channel deformation and allows for reversible bonding. The use of PDMS for bonding PMMA layers is an innovative approach, as it combines the advantages of PDMS's flexibility with PMMA's rigidity and optical clarity. Prior to bonding the microfluidic device, the devices were first gently washed with methanol and dried at 50 °C. subsequently, the aptasensor chambers in bottom layer were filled with a laser cutted aptasensors and ensures the alignment of the microchannel to the PSi. Finally, the chip was sealed with clamps and screws, ensuring leak-free operation.

2.5 PSi Layer Characterization

Specific structural properties i.e., thickness and morphology of the PSi samples was carried out using a field emission scanning electron microscopy (FE-SEM; MIRA3, TESCAN, Czech Republic) working at 15 kV acceleration voltage of the electron gun. Pores diameter distribution was obtained by ImageJ software (ImageJ; National Institutes of Health, Bethesda, MD, USA). The chemical modifications of the surface were verified with attenuated total reflectance Fourier transform infrared (ATR-FTIR) spectroscopy (UATR 2, PerkinElmer, USA) in the wavenumber range 400–4,000 cm^{-1}. Background and all sample spectra were measured in dry air and utilizing a diamond detector.

2.6 Measurement of Interferometric Reflectance Spectra

RIFTS method was used to monitor the reflectivity in real time changes of the PSi-based aptasensor. RIFTS measurements apparatus was undertaken as previously reported in ref. [12]. The spectral acquisition and the motorized xyz stage movement were controlled with a LabView software (National Instruments). The RIFTS method involved capturing reflectivity spectra and analyzing them using fast Fourier transformation (FFT) in the wavelength range of 450–900 nm. The FFT analysis revealed a single prominent peak representing the effective optical thickness (EOT) of the porous silicon layer. The EOT expressed as 2nL, where n represents the average refractive index of the PSi layer, and L denotes its physical thickness. Thus, a change in the latter indicates a change in the refractive index. The response data are presented as relative ΔEOT, defined as:

Equation 1

$$Response = \frac{\Delta EOT}{EOT_0} = \frac{EOT_t - EOT_0}{EOT_0}$$

EOT_0 represents baseline EOT value in PBS buffer, while EOT_t represents average EOT value at equilibrium after protein incubation, and washing procedures.

2.7 Biosensing and Selectivity Experiments

For the multiplexing capability and selectivity of the microfluidic aptasensor, we implemented a comprehensive testing protocol. Each of the three channels was functionalized with a distinct aptamer. The experimental procedure began with a 40-minute wash of the microchannels using PBS buffer allowed the aptamers to properly fold into their active 3D structures and established the initial EOT baseline. Subsequently, we introduced protein samples, including BSA (1 mg/mL), CRP (10 µg/mL), TNF-α (500 pg/mL), and IL-6 (500 pg/mL), both individually and as a mixture, for a duration of 50 minutes. After sample introduction, the surface was washed with PBS buffer for 10 minutes to remove unbound proteins. Throughout all steps, the flow rate maintained a consistent of 100 µL/min.

3. RESULT AND DISCUSSION

3.1 Characterization of PSi.

The FE-SEM analysis reveal the morphologies of the PSi layer i.e., thickness and pore size. Fig. 1a presents a top-view micrograph of the porous silicon surface, revealing the intricate network of pores and their distribution. The inset plot illustrates the pore size distribution, which ranges from 5 to 100 nm, with a predominant peak centered at 45 nm. The cross-sectional image of PSi provided in Fig. 1b shows the thickness of the resulting porous thin films, is about 3.80 µm and their morphology is characterized by cylindrical and typical aligned pores.

The ATR-FTIR analysis monitored surface chemistry undergoes a substantial change during the surface modification. Fig. 1c presents the FTIR spectral profiles corresponding to each stage of the surface modification process. Chemical functional groups in molecules are vibrated in distinct frequency areas as reflected in FTIR spectral. After oxidation, Si-H stretching vibrational frequencies at about 2100 cm^{-1} disappeared, however Si-O-Si bonds appeared at about 1050 cm^{-1}. Moreover, the broad absorption at 3360-3620 cm^{-1} is characteristic of the axial deformation of Si-OH. Following aptamer conjugation was verified by multiple characteristic DNA bands appear between 1720, 1260 and 870 cm^{-1}, attributed to the carbonyl groups stretching, phosphate stretching and saccharides vibrations, respectively. These results are similar to those reported by other [12-14].

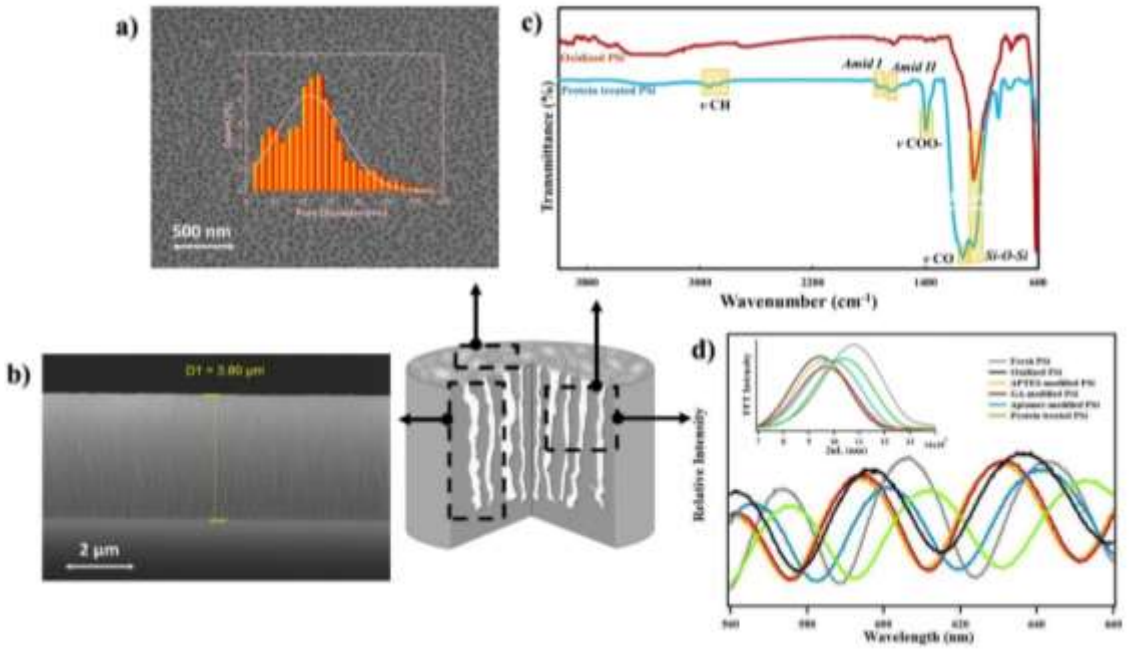

Fig. 1. PSi layer characterization. (a) top-view and (b) cross-section FESEM micrograph of the PSi layer (secondary electrons imaging). Inset in (a) pore diameter distribution. (c) ATR-FTIR spectra of oxidized PSi (red) and protein treated PSi (blue). (d) RIFTS method (inset: corresponding FFT values).

The RIFTS technique employed to verify each step of the PSi fabrication and modification process. Fig. 1d presents the reflectance spectra and Fourier transforms of the PSi during fabrication, oxidation and surface modification. Fourier transforms results in a single peak, indicated position along the x-axis equals the EOT of the porous layer and is linearly correlated to the refractive index changes of the PSi. The oxidation step resulted in an EOT increase from 50.59 ± 0.10 µm to 54.46 ± 0.21 µm, indicating the formation of a thin SiO2 layer on the pore surfaces and a consequent decrease in refractive index compared to the silicon skeleton. Subsequent surface modifications with 3-aminopropyltriethoxysilane and glutaraldehyde further increased the EOT to 56.48 ± 0.22 µm and 67.46 ± 0.35 µm, respectively. These increments signify an increase in refractive index and the successful formation of the organosilane layer. Finally, aptamer attachment further elevated the EOT to 92.09 ± 0.79 µm.

3.2 Microfluidic Design and Integration with PSi Films

The multiplex microfluidic device design is presented in Fig. 2a Each device contains three separate microchannels, spaced out at 4.0 mm apart, with a width of 1 mm and height of 60 µm. The aptasensor chamber along each channel with a width of 1 mm, length of 8 mm and height of 550 µm for placing of cutted aptasensor. This innovative microfluidic chip design ensures that only precisely cut porous silicon pieces contact the sample fluid. This approach optimizes cost-efficiency by reducing silicon consumption while allowing selective use of segments with optimal reflection spectra. Moreover, the microfluidic channel geometry was sensibly designed and simulated to ensure uniform fluid distribution. Simulation data confirm that the sample fluid reaches the aptasensor surfaces in all three channels simultaneously and with equal flux. This optimized flow pattern enhances the reliability and comparability of biomarker detection across channels, crucial for accurate multiplexed analysis.

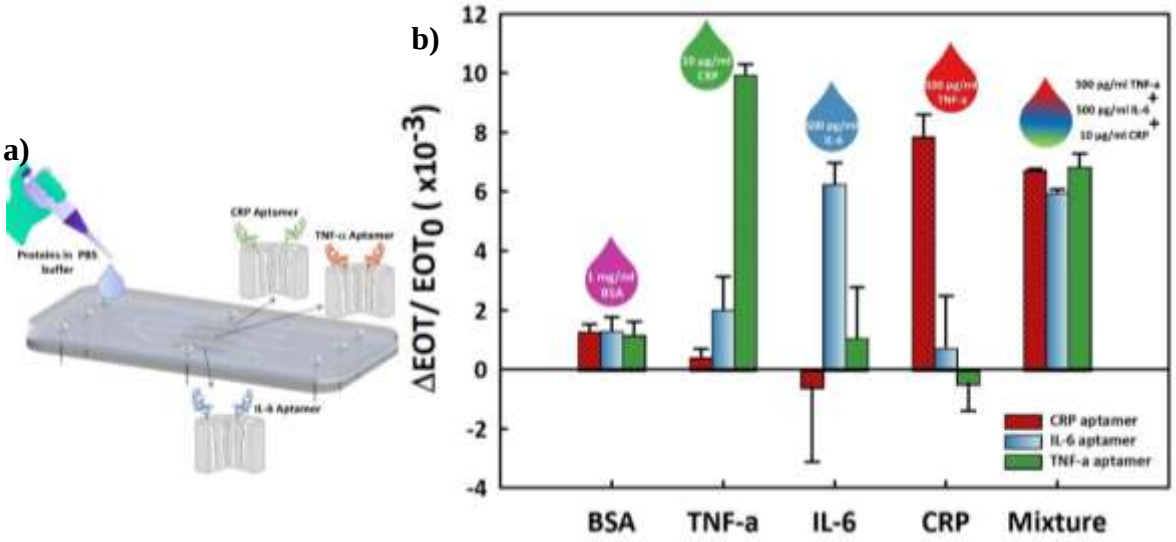

Fig. 2 (a) Schematic illustration of the multiplex microfluidic chip integrated with porous silicon interferometric aptasensor. (b) response upon exposure of the aptasensor to target and different nontarget protein solutions in PBS buffer.

3.3 Biosensing and Selectivity Experiments

To evaluate the multiplex and selective biosensing performance of the integrated platform, we incorporated three distinct aptasensor elements into the microfluidic biosensing chip. Each aptasensor was functionalized with a specific aptamer targeting one of three key biomarkers: CRP, TNF-α, and IL-6. The Fig. 2b illustrates the relative EOT changes of the PSi aptasensor upon the introduction of target and non-target proteins. Initially, the selectivity of the aptasensor was evaluated by exposing it to physiologically relevant non-target proteins, such as BSA, and observing its response. Additionally, recognizing that biosensors must function concurrently in the same environment and under identical conditions, we examined the cross-effect of CRP, IL-6, and TNF-a, both individually and in combination, on the performance of the aptasensors. The aptasensor exhibited high selectivity, detecting non-target proteins with minimal variations in the EOT signal and displaying consistent responses in the calibration curves to its specific target protein, whether alone or mixed with other biomarkers. Given that selectivity is essential for precise detection and differentiation of diseases in biological fluids, including blood, as it minimizes false positives and enhances resolution, the RIFTS technique successfully detected three biomarkers simultaneously and demonstrated high specificity despite the presence of non-specific biomolecules.

4. CONCLUSION

Multiplexing in point-of-care biosensors has revolutionized diagnostics across various fields, including medicine, environmental monitoring, and the food safety, by enabling rapid and simultaneous analysis of multiple analytes. In clinical settings, this technology is particularly crucial for multifactorial, multistage, and potentially fatal conditions like sepsis, a major cause of mortality in intensive care units. Consequently, the development of rapid, accurate, and multiplexed detection methods for sepsis-related biomarkers is crucial for timely diagnosis and informed treatment decisions.

This study focuses on designing and constructing a label-free aptasensor platform based on porous silicon, utilizing a 3-channel microfluidic system. The platform employs RIFTS technique to simultaneously identify three biomarkers. we synthesized, oxidized, and precisely laser cut porous silicon substrates. The surface chemistry was then modified using APTES and glutaraldehyde to facilitate aptamer bioconjugation. Each porous silicon piece was functionalized with a specific aptamer corresponding to one of the target sepsis biomarkers and subsequently integrated into a designed 3-channel microfluidic chip. A microcontroller-programmed motorized xyz stage enables precise, real-time monitoring across the reading points in channels simultaneously. The aptasensor was then exposed to various concentrations of samples containing CRP, TNF-α, and IL-6 biomarkers, both individually and in combination.

Performance evaluation using the RIFTS method demonstrated that the sensor is sensitive to concentration changes proportional to the biomarkers' dimensions and the resulting changes in refractive index. By

employing a 60 μm channel height, reducing the reaction rate in the microfluidic system, and considering the pore dimensions relative to the biomarkers (which are key factors in analyte diffusion within the pores), this chip shows promise for accurate detection of CRP, IL-6, and TNF-α biomarkers at high concentrations. This innovative integration allows for Comprehensive, multiplex and selective detection of multiple biomarkers, potentially enhancing the speed and accuracy of diagnosis applications.

REFERENCES

1. *Wang, J., et al., Silicon-Based Integrated Label-Free Optofluidic Biosensors: Latest Advances and Roadmap. Advanced Materials Technologies, 2020.* ***5****(6): p. 1901138.*
2. *Luppa, P. and R. Junker, Point-of-care testing: Principles and Clinical Applications. 2018: Springer.*
3. *Ehrmeyer, S.S. and R.H. Laessig, Point-of-care testing, medical error, and patient safety: a 2007 assessment. 2007.*
4. *Adamcova, M. and F. Šimko, Multiplex biomarker approach to cardiovascular diseases. Acta Pharmacologica Sinica, 2018.* ***39****(7): p. 1068-1072.*
5. *Mathur, S. and J. Sutton, Personalized medicine could transform healthcare. Biomedical reports, 2017.* ***7****(1): p. 3-5.*
6. *Faix, J.D., Biomarkers of sepsis. Critical reviews in clinical laboratory sciences, 2013.* ***50****(1): p. 23-36.*
7. *Raveendran, A.V., A. Kumar, and S. Gangadharan, Biomarkers and newer laboratory investigations in the diagnosis of sepsis. The journal of the Royal College of Physicians of Edinburgh, 2019.* ***49****(3): p. 207-216.*
8. *Teggert, A., H. Datta, and Z. Ali, Biomarkers for point-of-care diagnosis of sepsis. Micromachines, 2020.* ***11****(3): p. 286.*
9. *Sánchez-Salcedo, R., P. Sharma, and N.H. Voelcker, Advancements in Porous Silicon Biosensors for Point of Care, Wearable, and Implantable Applications. ACS Applied Materials & Interfaces, 2025.*
10. *Kumar, D.N., et al., Botulinum Neurotoxin C Dual Detection through Immunological Recognition and Endopeptidase Activity Using Porous Silicon Interferometers. Analytical Chemistry, 2022.* ***94****(15): p. 5927-5936.*
11. *Arshavsky Graham, S., et al., Mass transfer limitations of porous silicon-based biosensors for protein detection. ACS sensors, 2020.* ***5****(10): p. 3058-3069.*
12. *Yaghoubi, M., et al., A lectin-coupled porous silicon-based biosensor: label-free optical detection of bacteria in a real-time mode. Scientific Reports, 2020.* ***10****(1): p. 16017.*
13. *Arshavsky-Graham, S., et al., Aptamers vs. antibodies as capture probes in optical porous silicon biosensors. Analyst, 2020.* ***145****(14): p. 4991-5003.*
14. *Mello, M.L.S. and B. Vidal, Changes in the infrared microspectroscopic characteristics of DNA caused by cationic elements, different base richness and single-stranded form. 2012.*